Available online at www.sciencedirect.com

ScienceDirect

Proceedings of the Combustion Institute 38 (2021) 1053–1061

Proceedings of the Combustion Institute

www.elsevier.com/locate/proci

Automatic identification and lumping of high-temperature fuel decomposition pathways for chemical kinetics mechanism reduction

Lara Heberle*, Perrine Pepiot

Sibley School of Mechanical and Aerospace Engineering, Cornell University, Ithaca, NY 14853, United States

Received 8 November 2019; accepted 28 June 2020
Available online 19 September 2020

Abstract

The predictive capabilities of Computational Fluid Dynamics (CFD) for combustion systems rely on a proper description of the fuel chemistry. The growing interest in accurately capturing the combustion behavior of multi-component fuel mixtures creates additional challenges in developing reduced-order chemical kinetics mechanisms small enough to be used in CFD. Among the suite of chemistry reduction approaches available, lumping techniques appear especially suited to handle the complex nature of multi-component combustion chemistry. In particular, published literature provides very strong evidence that the lumping of non-rate-limiting pathways, and more specifically, the high-temperature fuel decomposition reactions, is a powerful avenue for multi-component mechanism reduction. In this work, we present a novel algorithm to identify and lump high temperature fuel decomposition reactions from detailed kinetic mechanisms. The lumping strategy is fully automatic, and relies exclusively on information available in the detailed mechanism. The performance of the technique is assessed for both a single-component fuel, *n*-dodecane, and its mixture with *iso*-octane. Results show that replacing the fuel decomposition sub-mechanism by a small number of reactions involving a single equivalent fuel component introduces very limited changes in the prediction of laminar flame speeds, ignition delay curves, and species profiles. This establishes a clear potential for the proposed algorithm to become a valuable addition to existing multi-stage mechanism reduction software.

Keywords: Kinetic mechanism reduction; Reaction lumping; High temperature chemistry; Multi-component fuels

1. Introduction

Mechanism reduction techniques are a powerful tool in decreasing prohibitively high CPU costs in predictive CFD simulations of practical combustion devices. These techniques can often be categorized into skeletal reduction (*e.g.* species and reaction elimination), time-scale reduction, and lumping techniques. Lumping, the focus of this paper, is especially attractive when dealing with high molecular weight hydrocarbon chemistry, for example in the fields of combustion, atmospheric chemistry, or oil processing, where a large number of isomers and similar reaction pathways are

* Corresponding author.
E-mail address: lcb96@cornell.edu (L. Heberle).

https://doi.org/10.1016/j.proci.2020.06.328

typically found. A variety of lumping approaches have been published in the literature, targeting reduction in different ways:

- Species lumping aims at replacing a set of species by a small number of representative variables, typically a single lumped species. While mathematical criteria have been devised to formulate lumping transformations, it is often performed in an *ad-hoc* manner based on chemical considerations, for example by lumping together isomer species with similar kinetic pathways, or by grouping species with similar chemical classes and functional groups [1,2].
- Lumping of reaction pathways, on the other hand, replaces a succession of elementary steps with a single lumped reaction and has the potential to forego intermediate species altogether. Hydrocarbon, and especially aliphatic fuel combustion chemistry, is particularly well-suited for this approach: because the fuel molecules undergo rapid oxidative pyrolysis at high temperature to form low molecular weight fragments, the fuel decomposition chemistry can be decoupled from small-species chemistry and lumped. This decoupling assumption has been used extensively in literature (e.g., [3,4]), the cut-off separating small radicals that govern the combustion dynamics from large species with limited influence on global combustion characteristics often being set to 4 carbon atoms.

Focusing here on combustion applications, lumping techniques have not only been used to reduce existing detailed kinetic mechanisms, but also as a powerful tool to directly generate simplified reaction schemes. For example, Ranzi et al. [5] defined a number of primary propagation reactions and radicals for a given fuel, and used those to create a simplified set of lumped fuel breakdown reactions. Recently, Wang et al. [6] proposed an approach using experimental data to define and calibrate small sets of lumped reactions to describe the high-temperature decomposition of transportation fuel mixtures. Again, those reactions were appended onto a detailed $C_0 - C_4$ kinetic mechanism, yielding chemical models of reasonable sizes, even for complex realistic fuels.

A significant drawback to many of the lumping techniques described above is the need for expert knowledge in defining the lumping transformation, selecting rate constants, classifying reactions, or identifying the sub-mechanism containing the reactions or species to lump. In this work, we aim to address those issues in the context of detailed kinetic mechanism reduction for high temperature combustion by developing an automated simulation-driven algorithm for the identification and lumping of fast fuel decomposition reactions, both in the context of single and multi-component fuel combustion. A flowchart of the proposed algorithm is available in the Supplemental Material (Fig. S1).

2. Lumping methodology

2.1. Overview and definitions

Fuel decomposition reactions in a detailed kinetic model describe the successive breakdown of large molecules into small hydrocarbon fragments. At high temperatures, fuel breakdown often occurs rapidly, and the corresponding kinetics have been found to minimally impact the main combustion dynamics [7]. Our objective is to replace those breakdown reactions by a small set of automatically defined lumped reactions.

We define $\mathbb{R}_d$ as the set of reactions in a high-temperature kinetic mechanism. $\mathbb{R}_d$ is split into two subsets: a set of fuel decomposition reactions, $\mathbb{R}_f$, with cardinality $n^{\mathbb{R}_f}$, that describe how the fuel molecule progressively breaks down into smaller hydrocarbon fragments, and a set of all the other reactions, referred to as *core reactions*, $\mathbb{R}_c$. The species in the detailed mechanism can be split into three subsets: the set of large hydrocarbon intermediates formed in the fuel decomposition process, $\mathbb{S}_f$, the set of fuel components $\mathbb{S}_F$, and the set of all other species, which will be called *core species*, $\mathbb{S}_c$.

To generate a lumped mechanism, we replace $\mathbb{R}_f$ with a set of *lumped reactions* $\mathbb{R}_\ell$. We assume that lumped reactions are of the form:

$$F + R \rightarrow \nu_1 P_1 + \nu_2 P_2 + ..., \tag{1}$$

where F is a lumped fuel molecule that can represent a single- or multi- component fuel, R is an *optional* reactant, ν_i are stoichiometric coefficients, and P_i are products. R and P_i must be core species and represent small species consumed and produced in fuel decomposition reactions. Species in $\mathbb{S}_f$ are removed from the lumped mechanism, as they are assumed to break down rapidly to core species. A summary is provided in Fig. 1.

2.2. Formulation of lumped reactions

Identification of reactions to lump: The first step in the lumping procedure is to systematically identify the reactions $\mathbb{R}_f$ and species $\mathbb{S}_f$ that characterize the detailed fuel breakdown process. A detailed reaction is assigned to $\mathbb{R}_f$ if it contributes to the formation of a product P without $C - C$ bond reconfiguration at any point between the consumption of a fuel molecule and the formation of P. As motivated in the introduction and following literature practices, $\mathbb{S}_f$ is defined as the set of all intermediate decomposition species directly produced by F which have $n^C > 4$.

In a given reaction, a product P is considered to be directly formed by a reactant R if all the

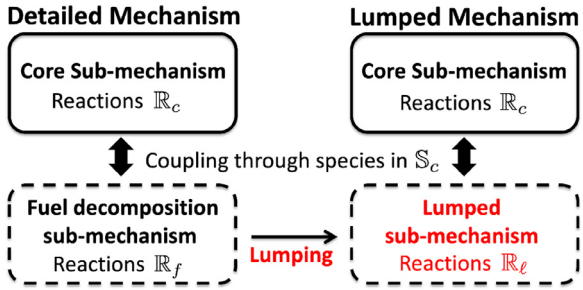

Fig. 1. Comparison of sub-mechanisms contained in detailed and lumped mechanisms.

carbon atoms in P are donated by R without rearrangement or combination with carbon atoms from other reactants. This is determined using transition state analysis described in [8], which detects the probability of carbon atoms in a given reactant to transfer to carbon atoms in a given product using structural and energy-based considerations.

Reference dataset Lumped reactions are formulated to minimize the difference between the production rate of core species from the detailed fuel decomposition reactions and that from lumped reactions, with an emphasis on predicting formation of species important to the core mechanism. For this purpose, a *reference dataset* of N samples is generated by recording chemical states over a series of detailed homogeneous auto-ignition simulations. Those configurations are recommended in Wang et al. [6] due to the clear separation in timescales between fuel decomposition and ignition.

A recorded dataset entry consists of the following stored variables: the temperature T, the concentration of species S_i, C_{S_i}, and the consumption and production rates of species involved in the fuel decomposition reactions, $\dot{C}^-_{S_i}$ and $\dot{C}^+_{S_i}$, respectively. $\dot{C}^-_{S_i}$ is computed as:

$$\dot{C}^-_{S_i} = \sum_{j=1}^{n^{\mathbb{R}_d}} \delta_j^{\mathbb{R}_f} \nu_{S_i}^{R_j} \omega_j \tag{2}$$

where ν^R refers to the reactant stoichiometric coefficients and ω_j, to the reaction rates. $\delta_j^{\mathbb{R}_f}$ is unity if the j^{th} reaction is in $\mathbb{R}_f$, 0 otherwise. $\dot{C}^+_{S_i}$ is computed as:

$$\dot{C}^+_{S_i} = \sum_{j=1}^{n^{\mathbb{R}_d}} \delta_j^{\mathbb{R}_f} \nu_{S_i}^{P_j} \omega_j \tag{3}$$

where ν^P refers to product stoichiometric coefficients. Concentration and consumption rates of the fuel are specifically denoted by C_F and $\dot{C}^-_F$. In the case of a multi-component fuel, these values are taken as the sum of contributions from each of the fuel components. An optional weighting factor, proportional to the size of the simulation time step when each entry was recorded, is also added to minimize sampling bias.

Entries are recorded for the duration of the oxidative fuel pyrolysis process in each reference simulation. Wang et al. [6] outlines the separation between oxidative fuel pyrolysis and oxidation of small molecules, concluding that the two processes can be separated temporally or spatially, and arbitrarily sets the cutoff between the two processes when the fuel is 95% decomposed in a shock tube study. Here, we define the decomposition process to occur while the fuel is driving the oxidative pyrolysis, that is, when the rate of fuel consumption exceeds the rate of consumption of any other large hydrocarbon.

Lumped reactions and reactants By construction, $\mathbb{R}_\ell$ contains two types of reactions: fuel decomposition and H-abstraction. We assume the presence of a uni-molecular fuel decomposition reaction to initiate fuel consumption, while H-abstraction reactions are added to $\mathbb{R}_\ell$ only if the consumption of a reactant $R \in \mathbb{S}_c$ relative to the consumption of fuel F in fuel decomposition reactions exceeds a user-defined cutoff α_-:

$$\frac{\sum_{n\in N} \left(\dot{C}^-_R\right)_n}{\sum_{n\in N} \left(\dot{C}^-_F\right)_n} \geq \alpha_- \tag{4}$$

Lumped reaction rate coefficients k and the Arrhenius parameters A and E are chosen so that, for each composition in the dataset, the *reactants' consumption rates* calculated using reactions in $\mathbb{R}_\ell$ are as close as possible to the values computed using the detailed set of fuel-related reactions, $\mathbb{R}_f$. This is done as follows:

- Entries in the reference dataset are first partitioned into a user-defined number of bins n_b based on the entry temperature. An average bin temperature T_b is then computed from all temperature entries in a given bin.
- For each temperature and each lumped reaction, the rate coefficient $k(T_b)$ is computed using a simple least squares approach over all entries in the bin. H-abstraction rate coefficients k_R are computed from reactant concentrations and the consumption rate of

reactant R recorded in the dataset as:

$$\dot{C}_R^- = k_R(T_b)C_F C_R \tag{5}$$

while decomposition rate coefficients k_F are computed from the fuel remaining after consumption in abstraction reactions:

$$\max\left(0, \dot{C}_F^- - \sum_{j=1}^{n^{\mathbb{R}_d}} \delta_j^R \dot{C}_R^-\right) = k_F(T_b)C_F \tag{6}$$

Once $k(T_b)$ is known for each lumped reaction, a 2-parameter Arrhenius fit, also based on a least square approach, is performed to obtain the corresponding reaction rate constants.

Lumped reaction products and product stoichiometric coefficients To define the lumped reaction products P_i and corresponding product stoichiometric coefficients ν_{P_i}, we impose several criteria: (1) each reaction must have a balanced number of elements, (2) all stoichiometric coefficients must be non-negative, and (3) the difference between the production rates of key fragments in lumped reactions and in detailed fuel decomposition reactions is minimized for species that are important to the core mechanism.

For lumped H-abstraction reactions with a radical R, we automatically select RH as a product to ensure elemental balance. Additional hydrocarbon products P_i are selected from the set of core species if their production in $\mathbb{R}_f$ relative to the production of other core species exceeds a user-defined cutoff α_+:

$$\frac{\sum_{n\in N}\left(\delta_F \dot{C}_{P_i}^+\right)_n}{\max_{s\in\mathbb{S}_c}\left(\sum_{n\in N}\left(\delta_F \dot{C}_s^+\right)_n\right)} \geq \alpha_+ \tag{7}$$

where $\delta_F = 1$ if the fuel consumption is at the maximum value for a given canonical simulation and is otherwise 0. This weighting ensures that products are selected at peak rates of fuel consumption, as selected products can significantly influence the rate of fuel decomposition.

Stoichiometric coefficients are computed with a weighted least squares fit to minimize the difference between all species production rates computed for lumped reactions and species production rates stored in the reference dataset. If a lumped product P_i is a reactant in any of the lumped reactions, ν_{P_i} is obtained from:

$$\dot{C}_{P_i}^+ = \sum_{j=1}^{n^{\mathbb{R}_d}} \delta_j^{\mathbb{R}_f} \nu_{P_{i,j}} \omega_j \tag{8}$$

where ω_j is the reaction rate of the jth lumped reaction, computed with Arrhenius parameters obtained with least squares fitting. Otherwise, ν_{P_i} is computed using the net rate of species formation:

$$\dot{C}_{P_i}^+ - \dot{C}_{P_i}^- = \sum_{j=1}^{n^{\mathbb{R}_d}} \delta_j^{\mathbb{R}_f} \nu_{P_{i,j}} \omega_j \tag{9}$$

In Eqs. (8) and (9), a weighting factor is applied to the least squares fits to weight any errors in the prediction of species production rates by the typical concentration of that species present in the system over all entries in the reference dataset. Least squares constraints are also imposed to enforce an elemental balance for every lumped reaction and to ensure that stoichiometric coefficients remain positive.

Lumped reaction parameter optimization As a optional final step, lumped reaction parameters can be adjusted so that the lumped mechanism better predicts key combustion phenomena of interest.

Adjusted parameters include the pre-exponential factor A and product stoichiometric coefficients ν_P. For each lumped reaction, A and all ν_P are combined to form a vector $\boldsymbol{\chi}$ of cardinality n^L, which is normalized to form the vector of active parameters $\mathbf{x}$ [9]:

$$\mathbf{x} = \ln\left(\frac{\boldsymbol{\chi}}{\boldsymbol{\chi}_0}\right)/\ln(\mathbf{F}) \tag{10}$$

where $\boldsymbol{\chi}_0$ is the nominal value of $\boldsymbol{\chi}$ and $\mathbf{F}$ is the uncertainty span of $\boldsymbol{\chi}$.

Parameters $\mathbf{x}$ are adjusted to minimize the difference between lumped model predictions $\eta(\mathbf{x})$ of quantities such as ignition delay time and laminar flame speed, computed with a second-order Taylor series expansion [10], and predictions of the same quantities η^{det} obtained with the detailed mechanism. The vector of optimal lumped reaction parameters $\mathbf{x}^*$ is computed via a solution mapping approach [9] to minimize the objective function Φ:

$$\Phi(\mathbf{x}^*) = \left(\sum_{i=1}^{n^T}\left(\frac{\eta_i(\mathbf{x}) - \eta_i^{\text{det}}}{\sigma_i \eta_i^{\text{det}}}\right)^2\right) \tag{11}$$

where n^T is the number of targets predictions to match and σ is a measure of target importance.

If all stoichiometric coefficient terms in $\mathbf{x}$ were perturbed independently during the computation of Taylor coefficients used to evaluate $\eta(\mathbf{x})$, elemental balances would not be maintained. Thus, for each atom type in each lumped reaction, we select a *constraining species* S to enforce an elemental balance. Stoichiometric coefficients of constraining species are not included in $\mathbf{x}$, and are instead automatically updated with element balances. Bounds are imposed on $\mathbf{x}$ to ensure that stoichiometric coefficients corresponding to both constraining species and species in the set of active parameters are non-negative.

3. Lumping of *n*-dodecane decomposition reactions

To assess the capabilities of the lumping methodology described above, we consider a high temperature *n*-dodecane mechanism consisting of 180 species and 1960 reactions [11]. The detailed

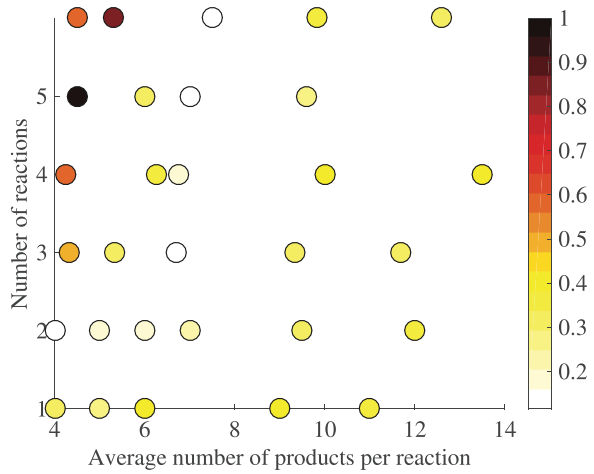

Fig. 2. Normalized ignition delay DTW error measure for a variety ($n^{\mathbb{R}_\ell}$, n^P) combinations, each corresponding to a specific (α_-, α_+) pair. Dark colors indicate larger discrepancies between detailed and lumped mechanism predictions.

reference dataset used to formulate the lumped reactions is assembled from a series of reference isochor auto-ignition simulations at stoichiometric conditions, at initial temperatures between 1100 and 1600 K, and pressures between 1 and 20 atm.

3.1. *Lumping parameter selection*

A parametric study is first conducted on the cut-off parameters α_- and α_+ used to determine the number of reactions and products in the lumped reactions. Both α_+ and α_- are varied between 0.01 and 1, yielding an ensemble of lumped sub-mechanisms containing between 1 (single decomposition reaction) and 6 (one decomposition reaction, 5 H-abstraction reactions) lumped reactions, each reaction containing between 4 and 14 products on average. Each is added to the core *n*-dodecane sub-mechanism and used to simulate the reference auto-ignition cases. An aggregate error measure for ignition delay time and species mass fraction profiles over all simulated configurations is then computed using the Fast Dynamic Time Warping (DTW) methodology [12], as implemented in Python's **fastdtw** package. In contrast to conventional point-wise error evaluations, DTW quantifies similarities between two curves with a single value, here the ignition delay times over a range of T_0 at a given p_0, and the species concentrations as function of time at a given p_0 and T_0, allowing for an efficient assessment of each lumped mechanism.

Figure 2 shows the DTW errors for each lumped mechanism, with magnitudes represented by marker color. For an easier understanding, α_- and α_+ are converted to the corresponding number of lumped reactions $n^{\mathbb{R}_\ell}$ and products n^P, and all DTW error values are normalized by the maximum value found over all ($n^{\mathbb{R}_\ell}$, n^P) combinations. A very similar picture is obtained for species profiles, and is available in the Supplementary Material (Fig. S2). While the magnitude of DTW errors is difficult to interpret, clear trends can be observed. More than one lumped reaction is required to properly capture the combustion dynamics. Furthermore, with too few products, the combustion process is not completely described, while too many products cause DTW errors to rise slightly as species with small production rates can be over-produced early in the combustion process. Accordingly, the cut-off values $\alpha_- = 0.02$ and $\alpha_+ = 0.2$. are selected, corresponding to 6 lumped reactions and 7.5 products per reaction on average.

3.2. n-*Dodecane lumped sub-mechanism*

With α_- and α_+ fixed, the lumping procedure is applied to fully describe reactants, products, product stoichiometric coefficients, and Arrhenius parameters for each lumped reaction. The various fits were found to be rather insensitive to the number of temperature bins used, with a value of 20 used throughout. The mechanism at the end of the lumping procedure contains 6 lumped reactions, 156 species, and a total of 1794 reactions. The fuel decomposition process is now described by 1 non-core species, down from 27 in the detailed mechanism, and 6 reactions, down from 176.

This mechanism is further adjusted using the optimization step described above. Representative ignition delays and integrated concentrations of lumped reactants and products are selected as the desired targets η. Ignition delays are assigned a value $\sigma = 0.05$, while integrated species concentration targets are assigned $\sigma = 1$. All elements in the uncertainty span vector **F** are set to 2.0, and a step

Table 1
Subset of lumped/optimized fuel decomposition reactions for the high temperature auto-ignition of *n*-dodecane/air and *n*-dodecane/*iso*-octane/air mixtures. Arrhenius parameters are in cm, s, mol, K, and kJ. Other reactants include H, O, CH_3 and HO_2.

n-Dodecane Lumped/optimized Reactions			A	E
n-$C_{12}H_{26}$ + OH	→	H_2O + 0.0263 H_2 + 1.3863 C_2H_4 + 0.2455 C_2H_5 + 1.5908 C_3H_6 + 0.1632 n-C_3H_7 + 0.3299 p-C_4H_8 + 0.5387 p-C_4H_9	1.90×10^{14}	17.19
n-$C_{12}H_{26}$	→	1.2912 C_3H_6 + 0.0367 n-C_3H_7 + 0.014 C_2H_5 + 0.38055 C_2H_4 + 0.1226 p-C_4H_8 + 1.6842 p-C_4H_9 + 0.13255 H_2	4.40×10^{16}	330.90
n-Dodecane/*iso*-octane Lumped/optimized Reactions			A	E
SUR + OH	→	H_2O + 0.193 CH_3 + 0.0278 H_2 + 0.0246 C_2H_4 + 0.2284 p-C_4H_9 + 0.1945 p-C_4H_8 + 0.0795 C_2H_5 + 1.013 C_3H_6 + 0.0594 n-C_3H_7 + 0.7884 i-C_4H_8 + 0.3841 t-C_4H_9	1.10×10^{14}	18.53
SUR	→	0.1177 CH_3 + 0.2028 H_2 + 0.0523 C_2H_4 + 0.4528 p-C_4H_9 + 0.1394 p-C_4H_8 + 0.3762 C_3H_6 + 0.2592 C_2H_5 + 0.1413 n-C_3H_7 + 0.7111 i-C_4H_8 + 0.6234 t-C_4H_9	1.72×10^{16}	310.82

size $\alpha = 0.5$ is used to generate the Taylor coefficients. Values for $\mathbf{F}$ and α were taken from similar previous studies [9,10]. $\boldsymbol{\chi}_0$ was set from the initial lumped model stoichiometric coefficients and Arrhenius rate parameters. Minimization of $\Phi(\mathbf{x})$ is performed using the global derivative-free method ISRES from the open-source library nLopt [13].

The final set of lumped/optimized reactions are shown in Table 1. Arrhenius parameters and stoichiometric coefficients are rounded to 2 and 4 significant figures respectively, except where more precision is needed for element balances. The mechanism containing lumped reactions with optimized parameters is hereafter referred to as the lumped/optimized mechanism. H_2 is selected as the H constraining species, p-C_4H_8 is selected as the C constraining species, and RH is selected as the O constraining species in reactions where radical R contains an oxygen atom.

3.3. n-*Dodecane lumped mechanism assessment*

Auto-ignition delay times are computed at the reference conditions and where experimental data is available. Comparisons for the latter are displayed in Fig. 3, showing very good agreement between lumped, lumped/optimized, and detailed predictions. Over the reference cases, 6% and 28% average errors are obtained between the lumped/optimized and detailed predictions, and between the lumped and detailed predictions, respectively. Laminar flame speeds computed with lumped and lumped/optimized mechanisms also found to compare favorably with the detailed mechanism and experimental results, as shown in Fig. 4 for *n*-dodecane-air mixtures at $p = 1$ atm and unburnt flame temperatures $T_u = 400$K and 470K.

In order to assess the predictions of time-dependent quantities, profiles of major species mole fractions are shown in Fig. 5 for a representative auto-ignition case with an average error in ignition delay time. While species mole fractions generated with the detailed mechanism are generally well-captured by the lumped/optimized mechanism, there is a slight over-prediction of some lumped products from basic mass conservation considerations due to the removal of species in $\mathbb{S}_f$. Note that pure pyrolysis cases are not included in the present analysis since they fall outside the range of conditions, all involving oxidative pyrolysis, used here to derive lumped reactions.

If fuel decomposition is fast compared to the chemical processes controlling the main ignition event, a key assumption of the proposed lumping approach, replacing its detailed description by a lumped one should not introduce any significant changes in the sensitivities and controlling processes of the system. Results of a sensitivity analysis for an isochor auto-ignition case with initial conditions $\phi_0 = 1$, $T_0 = 1400$ K, and $p_0 = 5$ atm are shown in Fig. 6. These results confirm that reactions in the detailed model with the greatest influence on autoignition delay time are indeed contained within the set of core reactions, as anticipated. More importantly, sensitivity coefficients of the most influential reactions are very similar for the detailed, lumped, and lumped/optimized mechanisms, indicating that lumping does not significantly alter core mechanism kinetics.

4. Lumping of a *n*-dodecane/*iso*-octane mixture

Finally, the lumping approach is applied to a two-component mechanism to demonstrate its capability in lumping both fuel components and fuel decomposition pathways. We consider a 50% *n*-dodecane/50% *iso*-octane mixture, with the corresponding mechanism obtained using the component library approach of Narayanaswamy et al. [18]. This mechanism contains 189 species and 1996 reactions.

The reference dataset is again generated with stoichiometric 0D isochor auto-ignition simulations, for $1100\,\text{K} < T_0 < 1600$ K, and $1\,\text{atm} < p_0 < 20$ atm. Cutoffs $\alpha_- = 0.02$ and

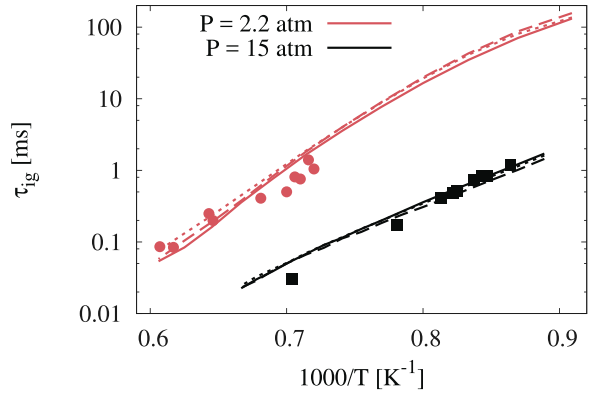

Fig. 3. Isochor ignition delays for detailed (solid lines), lumped (dotted lines), and lumped/optimized (dashed lines) mechanisms at high temperatures. Shock tube experiments (symbols) are by Davidson et al. [14] and Vasu et al. [15].

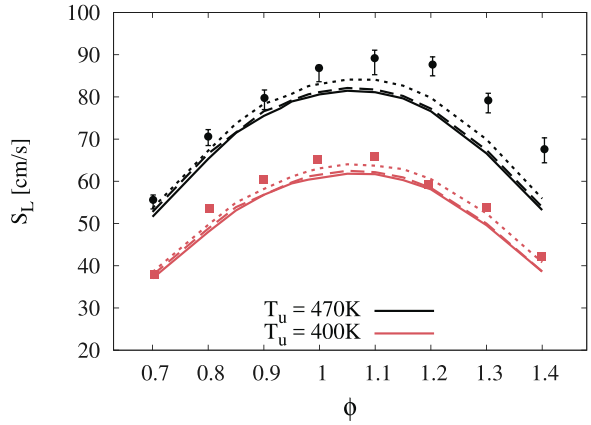

Fig. 4. Comparison of *n*-dodecane/air laminar flame speeds predicted using the detailed (solid lines), lumped (dotted lines), and lumped/optimized (dashed lines) mechanisms at the conditions corresponding to the experimental data (symbols, [16,17]).

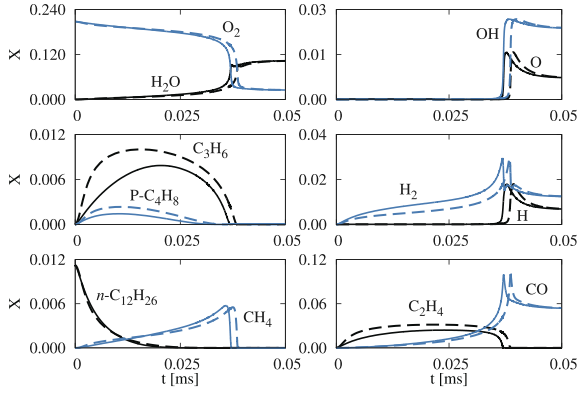

Fig. 5. Comparison of select species profiles obtained using the detailed (solid line) and lumped/optimized (dashed line) mechanisms for an isochor auto-ignition case with initial conditions $\phi = 1.0$, $p = 5$ atm, and $T = 1400$ K.

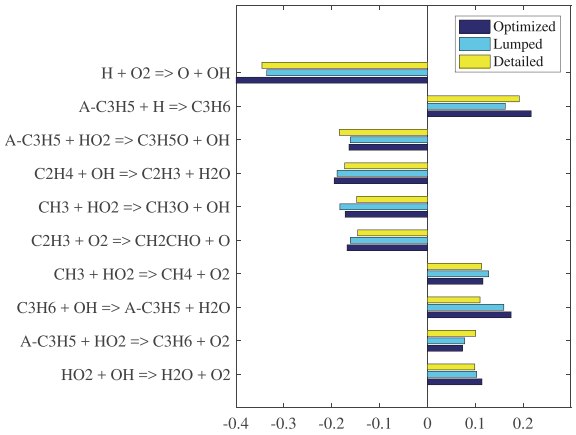

Fig. 6. Sensitivity coefficients of top 10 reactions controlling auto-ignition delay times for the detailed mechanism, compared to same reactions in the lumped and lumped/optimized mechanisms with initial conditions $\phi = 1.0$, $T = 1400$ K, and $p = 5$ atm. Sensitivity coefficients are computed by adjusting reaction rates by a factor of 2.0.

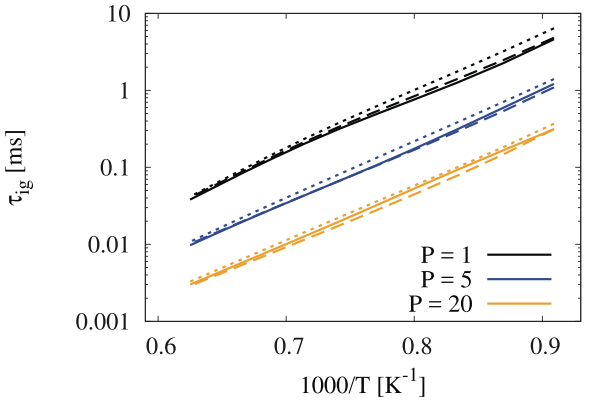

Fig. 7. Ignition delays for a 50% *n*-dodecane/50% *iso*-octane mixture at $\phi = 1$ and the reference dataset initial temperatures and pressures. comparison between detailed (Solid lines), lumped (dotted lines) and lumped/optimized (dashed lines).

$\alpha_+ = 0.1$ yield 6 lumped reactions with products from both *i*-octane and *n*-dodecane decomposition. Several of these are shown in Table 1, with the *n*-dodecane/*i*-octane fuel mixture treated as a single equivalent species "SUR". The mixing rules used to compute the equivalent thermochemical and transportation parameters for that species are described in [19]. The resulting lumped/optimized mechanism consists of 158 species and 1750 reactions.

Ignition delay times are shown in Fig. 7. The maximum ignition delay error computed with the lumped/optimized mechanism at conditions used to generate the lumped reactions is 13%, and the average ignition delay error is 7%. Error in laminar flame speeds (Fig. S3 in the Supplementary Material) are less than 3% for the same conditions as those of Fig. 4.

5. Conclusion

A novel approach is proposed to automatically lump high-temperature aliphatic fuel decomposition reactions in detailed mechanisms. Key features of this technique include the automated identification of the fuel decomposition sub-mechanism, the use of a reference database, and a fitting procedure complemented by a layer of optimization to determine the lumped kinetic parameters, bypassing entirely the need for user expertise. The methodology has been shown to successfully handle both single and multi-component fuel descriptions, replacing in the latter case the various fuel components by a single, equivalent species, and dramatically decreasing the size of the fuel decomposition sub-mechanism (e.g. a 96% decrease in the *n*-dodecane case). While the applicability of the methodology is currently limited to high

temperatures, the proposed algorithm has the potential to complement and significantly increase the performance of multi-stage mechanism reduction tools to obtain much needed CFD-tailored, multi-component reduced order kinetic models (an illustration for *n*-dodecane is provided in the Supplemental Material, while additional applications can be found in [19]). All mechanisms derived in this work are available as supplementary material.

Declaration of Competing Interest

None.

Acknowledgments

This work is supported in part by the US NSF under Grants DGE-1144153 and CBET-1653609.

Supplementary material

Supplementary material associated with this article can be found, in the online version, at doi:10.1016/j.proci.2020.06.328.

References

[1] P. Pepiot-Desjardins, H. Pitsch, *Comb. Theory and Model.* 12 (6) (2008) 1089–1108.
[2] L.A. Watson, D. Shall, S. Utembe, M. Jenkin, *Atm. Chem.* 42 (2008) 7196–7204.
[3] Y. Chang, M. Jia, Y. Li, Y. Liu, M. Xie, H. Wang, R.D. Reitz, *Combust. Flame* 162 (10) (2015) 3785–3802.
[4] C. Ji, E. Dames, Y.L. Wang, H. Wang, F.N. Egolfopoulos, *Combust. Flame* 157 (2) (2010) 277–287, doi:10.1016/j.combustflame.2009.06.011.
[5] E. Ranzi, M. Dente, A. Goldaniga, G. Bozzano, T. Faravelli, *Prog. Energy Comb. Sci.* 27 (2001) 99–139.
[6] H. Wang, R. Xu, K. Wang, C.T. Bowman, R.K. Hanson, D.F. Davidson, K. Brezinsky, F.N. Egolfopoulos, *Combust. Flame* 193 (2018) 502–519.
[7] Y. Gao, R. Shan, S. Lyra, C. Li, H. Wang, J.H. Chen, T. Lu, *Combust. Flame* 163 (2016) 437–446.
[8] C. Laurent, C. Frewin, P. Pepiot, *Combust. Flame* 173 (2016) 387–401.
[9] M. Frenklach, *Combust. Flame* 58 (1) (1984) 69–72.
[10] S.G. Davis, A.B. Mhadeshwar, D.G. Vlachos, H. Wang, *Int. J. Chem. Kinet.* 36 (2) (2003) 94–106.
[11] K. Narayanaswamy, P. Pepiot, H. Pitsch, *Combust. Flame* 161 (4) (2014) 866–884.
[12] S. Salvador, P. Chan, *Intel. Data Anal.* 11 (5) (2007) 561–580.
[13] S.G. Johnson, The nlopt nonlinear-optimization package, 2014.
[14] D. Davidson, Z. Hong, G. Pilla, A. Farooq, R. Cook, R. Hanson, *Proc. Comb. Inst.* 33 (1) (2011) 151–157.
[15] S. Vasu, D. Davidson, Z. Hong, V. Vasudevan, R. Hanson, *Proc. Comb. Inst.* 32 (1) (2009) 173–180.
[16] X. Hui, C. Sung, *Fuel* 109 (2013) 191–200.
[17] K. Kumar, C. Sung, *Combust. Flame* 151 (1) (2007) 209–224.
[18] K. Narayanaswamy, H. Pitsch, P. Pepiot, *Combust. Flame* 165 (2016) 288–309.
[19] L. Backer, *Generating reduced mechanisms for realistic multi-component fuel combustion*, Cornell University, 2019 Ph.D. thesis.